Journal of Soils and Sediments (2023) 23:3748–3760
https://doi.org/10.1007/s11368-023-03578-9

SOILS, SEC 1 • SOIL ORGANIC MATTER DYNAMICS AND NUTRIENT CYCLING • RESEARCH ARTICLE

Distribution and biodegradation of nonextractable polycyclic aromatic hydrocarbons in particle-size aggregates of field-contaminated soils

Ran Wei[1] · Shuting Wei[1] · Cheng Yao[1] · Weifeng Chen[1] · Liuming Yang[1] · Jinzhi Ni[1]

Received: 21 January 2023 / Accepted: 11 June 2023 / Published online: 21 June 2023
© The Author(s), under exclusive licence to Springer-Verlag GmbH Germany, part of Springer Nature 2023

Abstract

Purpose Adsorption on soil organic matter (SOM) and physical entrapment are the main mechanisms of nonextractable residue (NER) formation of polycyclic aromatic hydrocarbons (PAHs) in soil. Due to the SOM characteristics and pore structure in particle-size aggregates being different, the environmental fates of PAH NERs should be different as well. It's valuable to understand the distribution and biodegradation of PAH NERs in soil particle-size aggregates.

Materials and methods Three field-contaminated soils (Phaeozems, Anthrosols, and Calcareous soil) were separated into four particle-size aggregates (coarse sand, fine sand, coarse silt, and fine silt). The contents, compositions, and biodegradation of parent PAH NERs in particle-size aggregates were studied. Moreover, the effects of soil physico-chemical properties on the distribution and biodegradation of PAH NERs in particle-size aggregates were analyzed.

Results The percentages of PAH NERs to total PAHs in particle-size aggregates were in the range of 6.7–9.8%, 2.8–6.0%, and 24.3–35.9% for Phaeozems, Anthrosols, and Calcareous soil, respectively. Comparing with the composition of extractable PAHs, the proportions of two- and three-ring PAHs increased and five- and six-ring PAHs decreased of PAH NERs in all particle-size aggregates for each soil. Moreover, the proportions of PAH NERs decreased with the increase of PAH ring numbers overall. The contents of PAH NERs had significantly positive correlation with the contents of organic carbon (OC) ($p < 0.05$) in particle-size aggregates; however, the proportions of PAH NERs had significantly positive correlations with specific surface area, pore area, and volume ($p < 0.05$). The biodegradation rates of PAH NERs in particle-size aggregates were different in each soil and the degradation rates of total PAH NERs were lowest in Phaeozems owning to the highest OC content.

Conclusions The content of OC was the main factor controlling the distribution and biodegradation of PAH NERs in particle-size aggregates, and the entrapment in soil pores was the main factor controlling the proportions of PAH NERs. The proportions of PAH NERs were higher in low-molecular-weight PAHs than in high-molecular-weight PAHs. Our findings help deeply understand the environmental fates of PAH NERs in soils.

Keywords Polycyclic aromatic hydrocarbons · Field-contaminated soil · Nonextractable residues · Particle-size aggregates · Distribution · Biodegradation

1 Introduction

Polycyclic aromatic hydrocarbons (PAHs) are a class of persistent organic pollutants that are ubiquitous in the environment. Soil is a major reservoir for PAHs in the environment (Wild and Jones 1995). Great concerns on PAHs in soil are due to their carcinogenicity and mutagenicity that are threatening human health through direct contact and food chain (Costera et al. 2009).

After entering into soil, the bioavailability and extractability of PAHs decreased with increasing aging time (Ling

Responsible editor: Zhihong Xu

✉ Jinzhi Ni
nijz@fjnu.edu.cn

[1] Key Laboratory for Humid Subtropical Eco-geographical Processes of the Ministry of Education, Fujian Provincial Key Laboratory for Plant Eco-physiology, College of Geographical Science, Fujian Normal University, 350007 Fuzhou, Fujian, China

et al. 2010; Khan et al. 2012; Umeh et al. 2018a). During the aging processes, PAHs can form nonextractable residues (NERs) in soil that cannot be extracted by routine organic solvents and methods (Alexander 2000; Umeh et al. 2018a). The formation of NERs for parent or metabolite molecules of organic pollutants may result from chemical interactions with soil components and physical entrapment (Burauel and Führ 2000; Craven 2000).

Since the parent PAH compounds do not possess any coupling groups, the types of interactions that may be included in the formation of PAH NERs are van der Waals forces, charge-transfer complexes, hydrophobic partitioning, and physical trapping (sequestration) (Mordaunt et al. 2005). The mechanisms of PAH sequestration in soil include partitioning into soil organic matter (SOM) fractions such as fulvic and humic acid, humin, and SOM-mineral complexes within different particle-size aggregates, especially silt and clay (Doick et al. 2005; Duan et al. 2014; Eschenbach et al. 1998). Due to the components, chemical structure, and turnover time of SOM and physical structure of soil pores in different particle-size aggregates being different (Bol et al. 2009; Schulten and Leinweber 2000; Regelink et al. 2015; Liang et al. 2019; Li et al. 2020; Guidi et al. 2021), the formation and distribution of PAH NERs in them might also be different.

In the past work of research, the NERs of organic chemicals in soil were believed not having bioavailability and environmental threats to organisms, and the NER formation has been proposed as an substitute remediation approach for polluted soils (Alexander 2000; Berry and Boyd 1985). Though the NER formation decreases disclosure and consequently toxicity and threat of organic chemicals, it does not exclude exposure and threats. The PAH NERs were still considerably phytoavailable in field-contaminated soils (Gao et al. 2013, 2017). Umeh et al. (2018a) reported that benzo[a]pyrene (BaP) NERs could remobilize in soil, but the remobilized amounts significantly declined with aging time. Wang et al. (2017) also reported that much phenanthrene (Phe) NERs, particularly those physically sequestrated, were still bioavailable and might cause a toxic threat to soil organisms. After the exhaustion of the labile PAHs in a field-contaminated sediment, the nonlabile PAHs were transformed to the labile fraction with additional incubation for 30 days (Birdwell and Thibodeaux 2009). Remobilization and bioavailability have implications for the long-term fate of PAH NERs in soils as the related threats might be underestimated.

Many studies have reported the distribution of extractable PAHs in different particle-size aggregates in contaminated soils (Ni et al. 2008; Krauss and Wilcke 2002; Lu et al. 2012; Ray et al. 2012; Liao et al. 2013; Maqsood and Murugan 2017). To our knowledge, however, there are few studies about the distribution and biodegradability of PAH NERs in soil particle-size aggregates. Thus, the aims of this study are to elucidate (1) the distribution characteristics and composition of PAH NERs in soil particle-size aggregates; (2) the biodegradability of PAH NERs in different particle-size aggregates. The results of this study help to deeply understand the formation, bioavailability, and environmental fates of PAH NERs in field-contaminated soils.

2 Materials and methods

2.1 Chemicals

Acetonitrile (HPLC grade) was purchased from Merck & Co., Inc. Acetone (AR, ≥ 99.5%), dichloromethane (AR, ≥ 99.5%), hydrochloric acid (AR, 36.0–8.0%), sodium hydroxide (AR, ≥ 96.0%), and sodium sulfate anhydrous (AR, ≥ 99.0%) used in this study were bought from Sinopharm Chemical Reagent Co., Ltd., and organic solvents were redistilled before use. The standard mixture of 16 priority PAHs was bought from ANPEL Laboratory Technologies (Shanghai), Inc.

2.2 Soils

Three long-term PAH-contaminated soil samples were used in this study. The soil names were Phaeozems, Anthrosols, and Calcareous soil, and collected from a forest, liquid natural gas plant, and coking plant, respectively. The textures of Phaeozems, Anthrosols, and Calcareous soil are loam, sandy loam, and clayey loam, respectively, according to the international soil classification system. All soil samples were passed through a 2-mm metal sieve and thoroughly mixed and freeze-dried. The contents of soil organic carbon (OC) and total nitrogen (TN) were determined by elemental analysis at 1150 °C (Elementar Vario Max CN, Germany) after removing soil carbonate with 0.1 M HCl. Soil pH (soil: H_2O = 1:2.5) was determined with a glass electrode. Soil texture was measured by a laser particle size analyzer (Mastersizer 2000, Malvern Company, UK). Some of the soil's physico-chemical properties are listed in Table 1. The specific surface area (SSA) of the soil sample was measured by a Micro ASAP2020 SA analyzer using the Brunauer–Emmett–Teller (BET) nitrogen gas adsorption method. The parameters of the pore area and pore volume of the soil sample were also obtained from this measurement by using the BJH model (Table S1). The abbreviations of micropore, mesopore, macropore, and total pore area and volume were A_{micro}, A_{meso}, A_{macro}, A_{total}, V_{micro}, V_{meso}, V_{macro}, and V_{total}, respectively.

2.3 Soil particle-size fractionation

All soil samples were fractionated into four size aggregates, namely coarse sand (2000–250 μm), fine sand (250–54 μm),

Table 1 Physico-chemical properties of the tested soil samples

Soil samples		pH	OC ($g\ kg^{-1}$)	TN ($g\ kg^{-1}$)	C/N	Mass percentage (%)
Phaeozems	Bulk	5.15	45.95	3.66	12.6	-
	Coarse sand	-	54.20	4.58	11.8	51.7
	Fine sand	-	47.92	3.74	12.8	28.4
	Coarse silt	-	20.87	1.66	12.6	9.8
	Fine silt	-	32.64	3.64	8.9	10.1
Anthrosols	Bulk	4.21	24.01	0.85	28.4	-
	Coarse sand	-	17.83	0.32	56.5	29.5
	Fine sand	-	23.15	0.65	35.6	49.3
	Coarse silt	-	20.45	0.58	35.1	14.5
	Fine silt	-	22.35	1.35	16.6	6.7
Calcareous soil	Bulk	7.57	22.40	1.40	16.0	-
	Coarse sand	-	24.14	1.37	17.6	37.8
	Fine sand	-	23.44	1.51	15.5	35.5
	Coarse silt	-	20.16	0.93	21.6	9.2
	Fine silt	-	23.43	2.07	11.3	17.5

coarse silt (54–20 μm), and fine silt including clay (< 20 μm) according to the method of Ni et al. (2008) and Amelung et al. (1998) with some modifications. Briefly, 50 g of freeze-dried soil samples was dispersed in an ultrasonic bath (40 kHz, 200 W) for 30 min with a soil/water ratio of 1:5. Particle-size aggregates > 54 μm were separated by wet sieving with different mesh sieves and the aggregates < 54 μm were separated by a sedimentation method according to Stokes' law. All particle-size aggregates were lyophilized for further analysis. Soil mass recoveries of Phaeozems, Anthrosols, and Calcareous soil were in the range of 98.2–99.2% after particle-size fractionation.

2.4 Determination of extractable PAHs

The extractable PAHs in bulk soil and particle-size aggregates were determined according to the method of Richnow et al. (2000). Briefly, 2 g of freeze-dried soil sample was weighed precisely into a 40 mL PTFE centrifuge tube and firstly extracted with 10 mL acetone in an ultrasonic bath (40 kHz, 200 W) for 30 min, then centrifuged for 5 min at 4000 rpm; the supernatant was collected into a 100 mL round flask. Then, the soil sample was re-extracted as the same procedure above with one time of mixed solvent (dichloromethane: acetone = 1:1, v/v) and twice of dichloromethane. The supernatants of four extractions were combined and concentrated to ~ 1 mL by rotary evaporation. Then, 2 mL of acetonitrile was added and evaporated to ~ 1 mL twice solvent exchange to acetonitrile. For cleanup, extracts in acetonitrile were transferred to a C_{18} column (8 mm i.d.) filled with (from bottom up) glass wool, 3.5 cm of C_{18} (CNWBOND LC-C_{18}, 40–63 μm), and 1 cm of anhydrous Na_2SO_4, which was pre-eluted with 2 mL of acetonitrile. The column was then eluted with 5 mL of acetonitrile. The eluent was filtered with a 0.45 μm PTFE filter before analysis.

2.5 Determination of nonextractable PAHs

After removal of the extractable PAHs, all PTFE tubes were put in a fume hood to totally volatilize organic solvents left in soil samples. Then, the dried soil samples in the PTFE tubes were extracted to measure PAH NERs according to methods in the literature (Richnow et al. 2000; Gao et al. 2013; Umeh et al. 2018b) with some amendments. In brief, 10 mL of 2 mol•L^{-1} NaOH was added to each PTFE tube. The tubes were capped tightly and put in an oven at 100 ℃ for 2 h. The mixture in the tube was then centrifuged at 4000 rpm for 5 min. The supernatant was transferred to a clean PTFE tube. The soil residue was re-extracted with 2 mol•L^{-1} NaOH as above. The combined supernatant was then acidified to a pH less than 2 with 6 mol•L^{-1} HCl, and liquid–liquid extracted thrice with 10 mL dichloromethane each. The extracts in dichloromethane were condensed and cleaned as described above. The soil residue in the tube was lyophilized and extracted as the method of extractable PAHs. The total amounts of PAHs in the supernatant and soil residue were deemed as PAH NERs. The contents of extractable PAHs and PAH NERs in the three bulk soils are listed in Table S2.

2.6 Degradation of nonextractable PAHs in particle-size aggregates

High-efficiency degradation bacteria (*Agromyces* sp. PyB-10) isolated from a paddy soil using pyrene (Pyr) as a sole carbon source were used in the degradation experiment of PAH NERs. A 1.0 mL portion of the cell suspension at the concentration of 3×10^8 CFU·mL^{-1} was inoculated into a 50 mL PTFE tube containing 9 mL of MSM and 2 g (dry weight) of soil with only PAH NERs (i.e., soil residue after removing extractable PAHs with organic solvents). All tubes were incubated at 30℃ in the dark with shaking (220 rpm) for 30 days. Then, the mixture in all tubes was lyophilized and extracted with the method described in Sect. 2.5.

2.7 PAH analysis and quality control

The 15 US EPA priority PAHs were analyzed in this study. They were naphthalene (Nap), acenaphthene (Ace), fluorene (Flu), Phe, anthracene (Ant), Pyr, chrysene (Chry), fluoranthene (FluA), benzo[a]anthracene (BaA), dibenz[a,h]anthracene (DBA), BaP, benzo[k]fluoranthene (BkF), benzo[b]fluoranthene (BbF), benzo[g,h,i]perylene (BP), and indenol[1,2,3-cd]pyrene (IP). Acenaphthylene was excluded due to its weak fluorescence. The PAHs were determined by an ultra-performance liquid chromatography system (UPLC) (Waters Co., USA) coupled with a fluorescence detector using a reversed-phase column BEH Shield RP18 (150 mm × 2.1 mm, 1.7 μm). The specific method and quality control were provided in our previous study (Yang et al. 2023).

2.8 Calculations and statistical analysis

The percentages/proportions of PAH NERs in soil and particle-size aggregates for total and different-ring-number PAHs were calculated by the below formula:

$$\text{PAH NERs\%} = \frac{\text{PAH NERs}}{\text{PAH NERs} + \text{Extractable PAHs}} \times 100\% \quad (1)$$

The biodegradation rates of PAH NERs in soil and particle-size aggregates for total and different-ring-number PAHs were calculated by the below formula:

$$\text{Biodegradation rates (\%)} = \left(1 - \frac{\text{Contents of PAH NERs after biodegradation}}{\text{Contents of PAH NERs before biodegradation}}\right) \times 100\%$$

The statistical analysis was performed using SPSS 17.0. A significant level of correlation between two sets of data ($n = 12$) was evaluated by using Pearson's correlation test (two-tailed). One-way analysis of variance (ANOVA) with Tukey's HSD was used to identify significant differences between particle-size aggregates.

3 Results

3.1 Contents of extractable and nonextractable PAHs in particle-size aggregates

In Phaeozems, the average contents of total extractable PAHs in soil particle-size aggregates ranged from 13,851 to 40,364 μg·kg^{-1}, and decreased in the order of fine sand > coarse sand > fine silt > coarse silt (Table 2). The average contents of total PAH NERs in soil particle-size aggregates were in the range of 1119–3958 μg·kg^{-1} and had the same order as extractable PAHs (Table 2). The average percentages of PAH NERs to total PAHs in soil particle-size aggregates ranged from 6.7 to 9.8%, and decreased in the order of fine silt > fine sand > coarse silt > coarse sand (Table 2). According to the mass percentages and PAH contents of each soil particle-size aggregate, the average calculated mass distribution of extractable PAHs and PAH NERs were in the order of fine sand (59.8%) > coarse sand (29.7%) > coarse silt (6.1%) > fine silt (4.4%) and fine sand (65.3%) > coarse sand (23.9%) > coarse silt (5.4%) ≈ fine silt (5.4%), respectively.

In Anthrosols, the average contents of total extractable PAHs in soil particle-size aggregates ranged from 3016 to 6718 μg·kg^{-1} and increased with decreasing particle size, i.e., coarse sand < coarse silt < fine sand < fine silt (Table 3). The average contents of total PAH NERs in soil particle-size aggregates were in the range of 86–430 μg·kg^{-1} and had the same order as extractable PAHs (Table 3). The average percentages of PAH NERs to total PAHs in soil particle-size aggregates were highest in fine silt (6.0%) and the other three aggregates were nearly equal (2.8–3.0%) (Table 3). The average mass distribution of extractable PAHs and PAH NERs were in the order of coarse sand (40.7%) > fine sand (27.5%) > fine silt (17.8%) > coarse silt (14.0%) and coarse sand (32.5%) > fine silt (31.7%) > fine sand (24.0%) > coarse silt (11.8%), respectively.

In Calcareous soil, the average contents of total extractable PAHs in soil particle-size aggregates ranged from 2626 to 5689 μg·kg^{-1} and increased with decreasing particle size, i.e., coarse sand < coarse silt < fine sand < fine silt (Table 4). The average contents of total PAH NERs in soil particle-size aggregates were in the range of 1418–1992 μg·kg^{-1} and decreased in the order of fine sand > fine silt > coarse

Table 2 Contents of extractable and nonextractable PAHs in soil particle-size aggregates of Phaeozems (μg·kg^{-1})

PAHs	Coarse sand		Fine sand		Coarse silt		Fine silt	
	Extractable	NERs	Extractable	NERs	Extractable	NERs	Extractable	NERs
Nap	946 ± 103	309 ± 3	1331 ± 50	523 ± 44	495 ± 17	127 ± 0	911 ± 30	244 ± 26
Ace	832 ± 161	ND	680 ± 39	ND	63 ± 23	ND	162 ± 94	ND
Flu	488 ± 78	39 ± 2	530 ± 13	63 ± 3	160 ± 8	4 ± 1	274 ± 15	39 ± 5
Phe	4756 ± 786	467 ± 66	4843 ± 77	760 ± 65	1739 ± 13	222 ± 8	2739 ± 6	463 ± 41
Ant	737 ± 141	26 ± 0	692 ± 1	39 ± 3	185 ± 1	16 ± 0	251 ± 3	37 ± 3
FluA	6526 ± 816	627 ± 137	6861 ± 159	1116 ± 113	2422 ± 268	295 ± 21	3818 ± 641	516 ± 43
Pyr	3175 ± 444	70 ± 9	2851 ± 115	105 ± 20	1192 ± 30	42 ± 5	1858 ± 7	100 ± 5
BaA	2783 ± 396	274 ± 59	2998 ± 0	457 ± 73	1189 ± 22	135 ± 12	1917 ± 19	261 ± 27
Chry	2982 ± 510	55 ± 14	2704 ± 48	79 ± 1	1038 ± 18	25 ± 2	1561 ± 50	68 ± 4
BbF	2543 ± 454	219 ± 64	2762 ± 104	305 ± 34	1180 ± 3	48 ± 27	1784 ± 79	200 ± 5
BkF	1327 ± 204	33 ± 6	1175 ± 3	54 ± 2	475 ± 0	17 ± 2	760 ± 4	53 ± 1
BaP	2915 ± 445	80 ± 21	2665 ± 30	150 ± 1	1046 ± 0	48 ± 2	1614 ± 3	104 ± 4
DBA	340 ± 76	14 ± 9	278 ± 13	26 ± 10	116 ± 5	7 ± 0	186 ± 14	17 ± 2
BP	1508 ± 521	85 ± 26	8645 ± 1606	131 ± 5	1965 ± 9	66 ± 2	3147 ± 94	151 ± 32
IP	1616 ± 243	114 ± 47	1347 ± 83	149 ± 0	588 ± 35	67 ± 1	991 ± 58	140 ± 8
∑PAHs	33,474 ± 4469	2412 ± 462	40,364 ± 1370	3958 ± 280	13,851 ± 196	1119 ± 20	21,975 ± 765	2395 ± 122
NERs%	6.7 ± 0.4 c		8.9 ± 0.9 ab		7.5 ± 0.0 bc		9.8 ± 0.1 a	

Values are means ± standard deviation ($n = 3$); ND indicates below detection limit. In the last row, values followed by different letters denote the significant differences among particle-size aggregates according to Turkey's test ($p < 0.05$). NERs% was calculated by the formula of PAH NERs/(PAH NERs + Extractable PAHs) × 100%

sand > coarse silt (Table 4). The average percentages of PAH NERs to total PAHs in soil particle-size aggregates were in the range of 24.3–35.9% and decreased with decreasing particle size, i.e., coarse sand > coarse silt > fine sand > fine silt (Table 4). The average mass distribution of extractable PAHs and PAH NERs was in the order of fine sand

Table 3 Contents of extractable and nonextractable PAHs in soil particle-size aggregates of Anthrosols (μg·kg^{-1})

PAHs	Coarse sand		Fine sand		Coarse silt		Fine silt	
	Extractable	NERs	Extractable	NERs	Extractable	NERs	Extractable	NERs
Nap	78 ± 48	ND	161 ± 6	14 ± 1	179 ± 3	18 ± 1	167 ± 9	29 ± 1
Ace	ND	ND	ND	ND	ND	ND	ND	ND
Flu	10 ± 2	ND	37 ± 1	ND	78 ± 4	ND	85 ± 7	4 ± 6
Phe	185 ± 102	10 ± 4	321 ± 8	19 ± 3	625 ± 38	28 ± 2	615 ± 60	74 ± 0
Ant	18 ± 11	2 ± 0	39 ± 1	2 ± 0	54 ± 1	4 ± 1	51 ± 4	9 ± 0
FluA	315 ± 150	16 ± 2	670 ± 30	15 ± 2	1084 ± 14	28 ± 3	1138 ± 110	90 ± 2
Pyr	238 ± 96	13 ± 0	381 ± 29	20 ± 10	517 ± 4	25 ± 0	785 ± 44	46 ± 4
BaA	158 ± 19	6 ± 2	241 ± 10	8 ± 4	324 ± 7	10 ± 3	429 ± 17	23 ± 1
Chry	183 ± 25	2 ± 0	249 ± 14	2 ± 0	295 ± 6	2 ± 0	418 ± 18	9 ± 1
BbF	358 ± 19	6 ± 3	304 ± 7	6 ± 3	465 ± 36	8 ± 1	709 ± 26	22 ± 1
BkF	99 ± 2	3 ± 1	108 ± 7	5 ± 0	141 ± 4	5 ± 0	213 ± 10	9 ± 0
BaP	192 ± 29	7 ± 0	236 ± 19	8 ± 1	292 ± 15	8 ± 0	441 ± 17	17 ± 0
DBA	168 ± 90	ND	495 ± 188	ND	726 ± 296	12 ± 0	650 ± 106	68 ± 3
BP	316 ± 70	6 ± 0	244 ± 48	5 ± 0	366 ± 28	5 ± 0	460 ± 6	12 ± 2
IP	700 ± 188	13 ± 3	230 ± 32	11 ± 2	318 ± 2	12 ± 0	556 ± 178	17 ± 3
∑PAHs	3016 ± 117	86 ± 8	3715 ± 373	116 ± 14	5463 ± 316	165 ± 1	6718 ± 246	430 ± 10
NERs%	2.8 ± 0.1 b		3.0 ± 0.1 b		2.9 ± 0.2 b		6.0 ± 0.1 a	

Values are means ± standard deviation ($n = 3$); ND indicates below detection limit. In the last row, values followed by different letters denote the significant differences among particle-size aggregates according to Turkey's test ($p < 0.05$). NERs% was calculated by the formula of PAH NERs/(PAH NERs + Extractable PAHs) × 100%

Table 4 Contents of extractable and nonextractable PAHs in soil particle-size aggregates of Calcareous soil (μg·kg^{-1})

PAHs	Coarse sand		Fine sand		Coarse silt		Fine silt	
	Extractable	NERs	Extractable	NERs	Extractable	NERs	Extractable	NERs
Nap	192 ± 7	165 ± 3	305 ± 15	314 ± 81	338 ± 18	187 ± 29	570 ± 9	303 ± 27
Ace	ND	66 ± 9	ND	172 ± 27	ND	61 ± 27	ND	62 ± 8
Flu	31 ± 19	37 ± 5	68 ± 2	57 ± 5	84 ± 4	23 ± 2	152 ± 0	29 ± 1
Phe	471 ± 15	340 ± 19	683 ± 22	494 ± 67	826 ± 16	298 ± 12	1253 ± 21	357 ± 11
Ant	31 ± 1	25 ± 8	49 ± 1	57 ± 31	55 ± 1	20 ± 0	83 ± 0	25 ± 1
FluA	591 ± 24	420 ± 30	815 ± 40	501 ± 16	992 ± 33	428 ± 12	1272 ± 54	512 ± 13
Pyr	168 ± 27	72 ± 18	281 ± 19	56 ± 0	290 ± 14	74 ± 7	385 ± 30	96 ± 9
BaA	297 ± 31	173 ± 13	407 ± 22	147 ± 8	406 ± 8	133 ± 2	594 ± 1	172 ± 19
Chry	85 ± 10	10 ± 0	138 ± 12	12 ± 0	120 ± 3	13 ± 1	170 ± 6	29 ± 3
BbF	164 ± 15	53 ± 15	234 ± 20	54 ± 7	235 ± 27	76 ± 1	393 ± 7	94 ± 33
BkF	48 ± 4	8 ± 2	87 ± 9	11 ± 0	77 ± 1	11 ± 0	113 ± 1	18 ± 1
BaP	83 ± 10	18 ± 2	162 ± 26	18 ± 0	135 ± 5	16 ± 1	158 ± 2	23 ± 2
DBA	19 ± 1	6 ± 1	31 ± 2	6 ± 0	28 ± 0	4 ± 0	36 ± 0	9 ± 2
BP	231 ± 49	18 ± 2	412 ± 40	44 ± 1	365 ± 14	20 ± 2	231 ± 99	36 ± 2
IP	214 ± 52	63 ± 1	545 ± 211	49 ± 3	356 ± 21	52 ± 6	279 ± 27	59 ± 9
∑PAHs	2626 ± 91	1472 ± 99	4216 ± 60	1992 ± 197	4306 ± 83	1418 ± 72	5689 ± 11	1823 ± 126
NERs%	35.9 ± 2.4 a		32.0 ± 1.9 a		24.8 ± 1.3 b		24.3 ± 1.3 b	

Values are means ± standard deviation ($n = 3$); ND indicates below detection limit. In the last row, values followed by different letters denote the significant differences among particle-size aggregates according to Turkey's test ($p < 0.05$). NERs% was calculated by the formula of PAH NERs/ (PAH NERs + Extractable PAHs) × 100%

(38.5%) > fine silt (25.7%) ≈ coarse sand (25.6%) > coarse silt (10.2%) and fine sand (41.2%) > coarse sand (32.5%) > fine silt (18.7%) > coarse silt (7.6%), respectively.

3.2 Composition of extractable and nonextractable PAHs in particle-size aggregates

For the extractable PAHs in Phaeozems (Fig. 1A), four-ring PAHs were the dominant PAHs in all particle-size aggregates and ranged from 38.2 to 46.2%; two-ring PAHs were the lowest PAHs and ranged from 2.8 to 4.2%. The compositions of the extractable PAHs in all particle-size aggregates were generally similar with some exceptions. In coarse sand, the proportion of six-ring PAHs was significantly lower than that of all other aggregates and the proportion of four-ring PAHs was significantly higher than that of fine sand ($p < 0.05$). For the PAH NERs in Phaeozems (Fig. 1B), four-ring PAHs were also the dominant PAHs in all particle-size aggregates and ranged from 39.5 to 44.4%; three-ring PAHs were the second-highest concentration PAHs and ranged from 21.7 to 22.5%. The composition of PAH NERs in all particle-size aggregates was similar except for six-ring PAHs. The proportions of six-ring PAH NERs in coarse silt and fine silt were similar and significantly higher than that of fine sand ($p < 0.05$). Comparing with the composition of extractable PAHs, the proportions of two- and three-ring PAHs increased and those of five- and six-ring PAHs decreased for PAH NERs in all particle-size aggregates (Fig. 1).

For the extractable PAHs in Anthrosols (Fig. 2A), four-ring PAHs were the dominant PAHs in all particle-size aggregates except coarse sand and ranged from 29.5 to 41.6%; two-ring PAHs were the lowest PAHs and ranged from 2.5 to 4.4%. The compositions of the extractable PAHs in all particle-size aggregates were similar except for coarse sand. In coarse sand, six-ring PAHs were the dominant PAHs (33.9%) and their proportion was significantly higher than that in coarse silt ($p < 0.05$) (Fig. 2A). For the PAH NERs in Anthrosols (Fig. 2B), four-ring PAHs were also the dominant PAHs in all particle-size aggregates and ranged from 38.4 to 43.8%. The compositions of PAH NERs in fine sand and coarse silt were similar. In coarse sand, the proportions of six-ring PAH NERs were significantly higher than those of coarse silt and fine silt ($p < 0.05$). Moreover, two-ring PAH NERs were undetected in coarse sand (Fig. 2B). Comparing with the composition of the extractable PAHs, the proportions of two- and three-ring PAHs increased and five- and six-ring PAHs decreased in PAH NERs in general (Fig. 2).

For the extractable PAHs in Calcareous soil (Fig. 3A), four-ring PAHs were the dominant PAHs in all particle-size aggregates and ranged from 39.0 to 43.4%; two-ring PAHs were the lowest PAHs and ranged from 7.2 to 10.0%. The compositions of the extractable PAHs in all particle-size

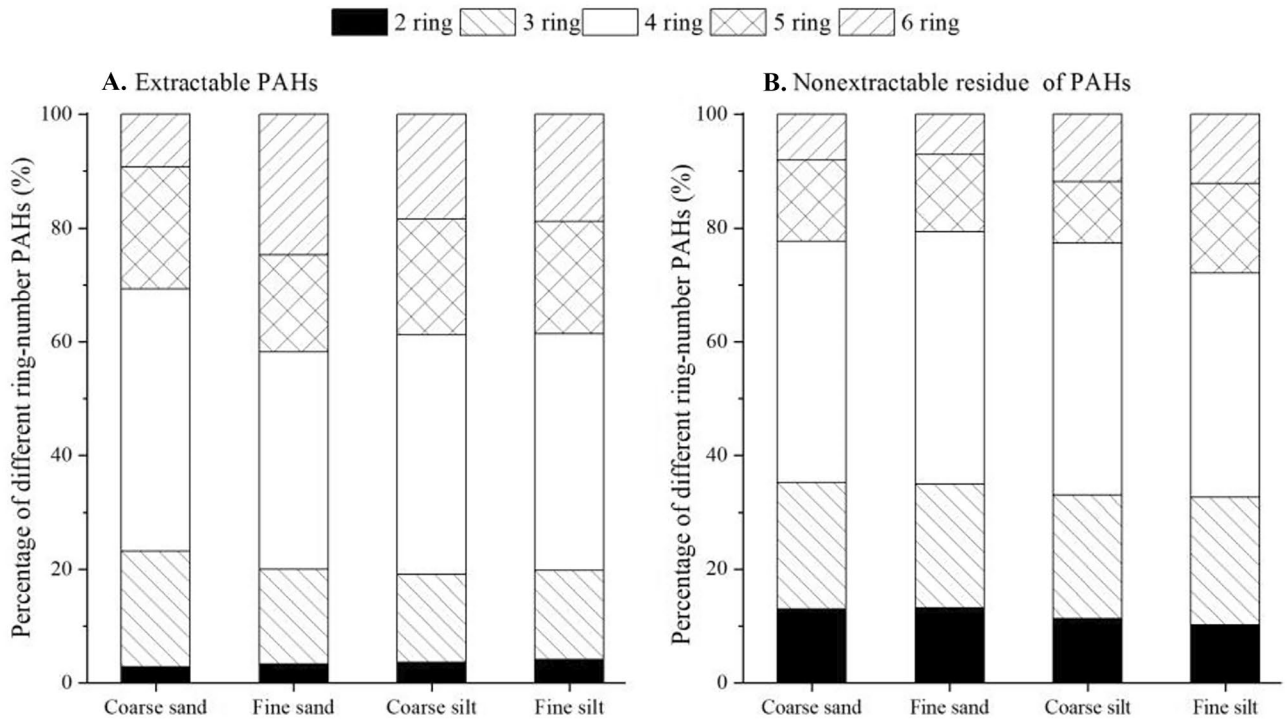

Fig. 1 Compositions of extractable and nonextractable PAHs in particle-size aggregates of Phaeozems

aggregates were very similar except for fine silt. In fine silt, the proportions of two- and three-ring PAHs were significantly higher than all other aggregates ($p < 0.05$), and six-ring PAHs were significantly lower than fine sand ($p < 0.05$) (Fig. 3A). For the PAH NERs in Calcareous soil (Fig. 3B), four-ring PAHs were also the dominant PAHs

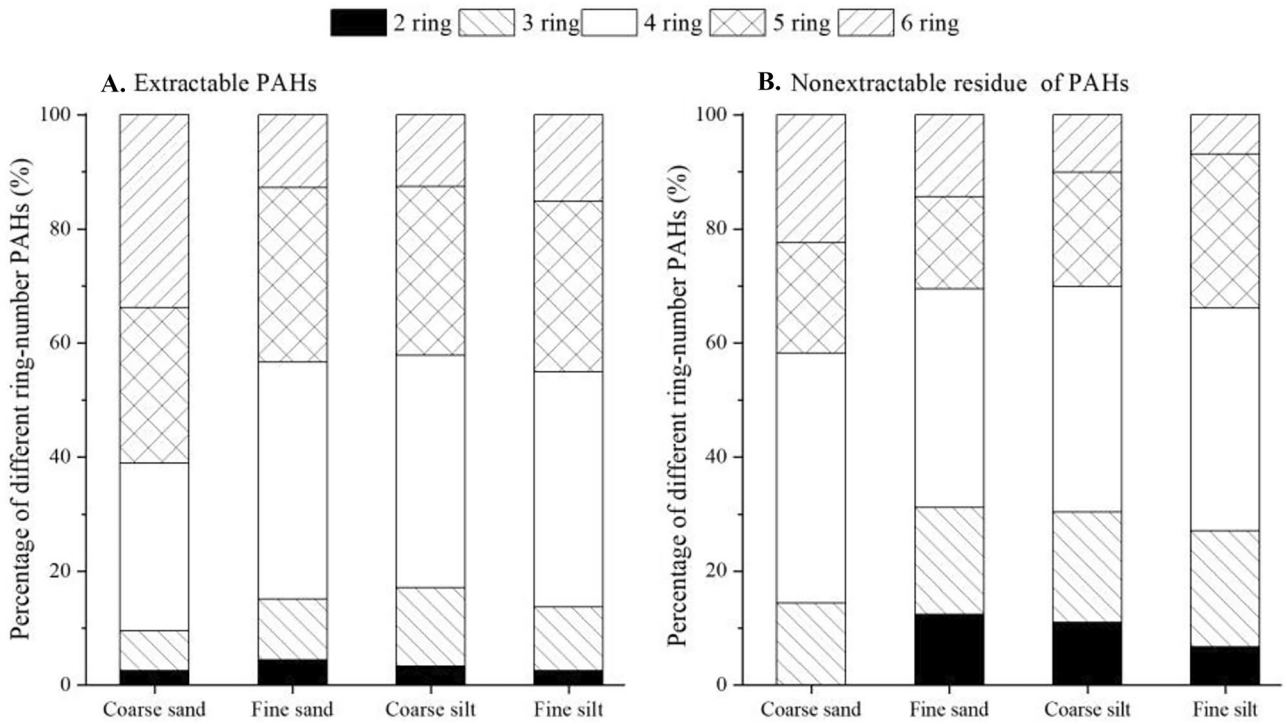

Fig. 2 Compositions of extractable and nonextractable PAHs in particle-size aggregates of Anthrosols

in all particle-size aggregates except fine sand and ranged from 36.2 to 45.8%; three-ring PAHs was the second-highest PAHs and ranged from 26.0 to 39.1%. The compositions of PAH NERs in all particle-size aggregates were similar except for fine sand. In fine sand, the proportion of three-ring PAHs was significantly higher than that in other aggregates ($p < 0.05$) (Fig. 3B). Comparing with the compositions of the extractable PAHs, the proportions of two- and three-ring PAHs increased and five- and six-ring PAHs decreased in PAH NERs in all particle-size aggregates (Fig. 3).

In order to explore the effect of ring numbers on the formation of PAH NERs in different particle-size aggregates, the proportions of PAH NERs to total PAHs in respect of different ring numbers were calculated, and the results are shown in Fig. 4. In all particle-size aggregates of the three soils, the average proportions of PAH NERs decreased with the increase of PAH ring numbers in general and the proportion of two-ring PAH NERs was especially higher than other ring number PAH NERs.

In Phaeozems (Fig. 4A), the proportion of two-ring PAH NERs in fine sand was significantly higher than that of coarse silt and fine silt. The proportions of three- and four-ring PAH NERs in coarse sand were significantly lower than those of fine sand and fine silt. The proportion of five-ring PAH NERs in fine silt was significantly higher than that of coarse sand and coarse silt. The proportion of six-ring PAH NERs in fine sand was significantly lower than that of coarse sand and fine silt.

In Anthrosols (Fig. 4B), the proportions of PAH NERs with different ring numbers in fine silt were all significantly higher than those of other particle-size aggregates in general ($p < 0.05$) except six-ring PAH NERs that was no significant difference among the four particle-size aggregates. There were no significant differences in the proportions of PAH NERs with different ring numbers among the other three particle-size aggregates except that the proportion of four-ring PAH NERs in coarse sand was significantly higher than that of fine sand and coarse silt ($p < 0.05$).

In Calcareous soil (Fig. 4C), there were no significant differences in the proportions of PAH NERs with different ring numbers among all particle-size aggregates except that the proportions of three- and four-ring PAH NERs in coarse sand and three-ring PAH NERs in fine sand were significantly higher than those of in coarse silt and fine silt ($p < 0.05$).

3.3 Biodegradation of nonextractable PAHs in soil particle-size aggregates

In Phaeozems, the average degradation rates of total PAH NERs in the four particle-size aggregates were all negative (Fig. 5A). In respective of different-ring-number PAHs, the average degradation rates of five- and six-ring PAH NERs in coarse sand and fine silt and six-ring PAH NERs in fine sand and coarse silt were positive, and the average degradation

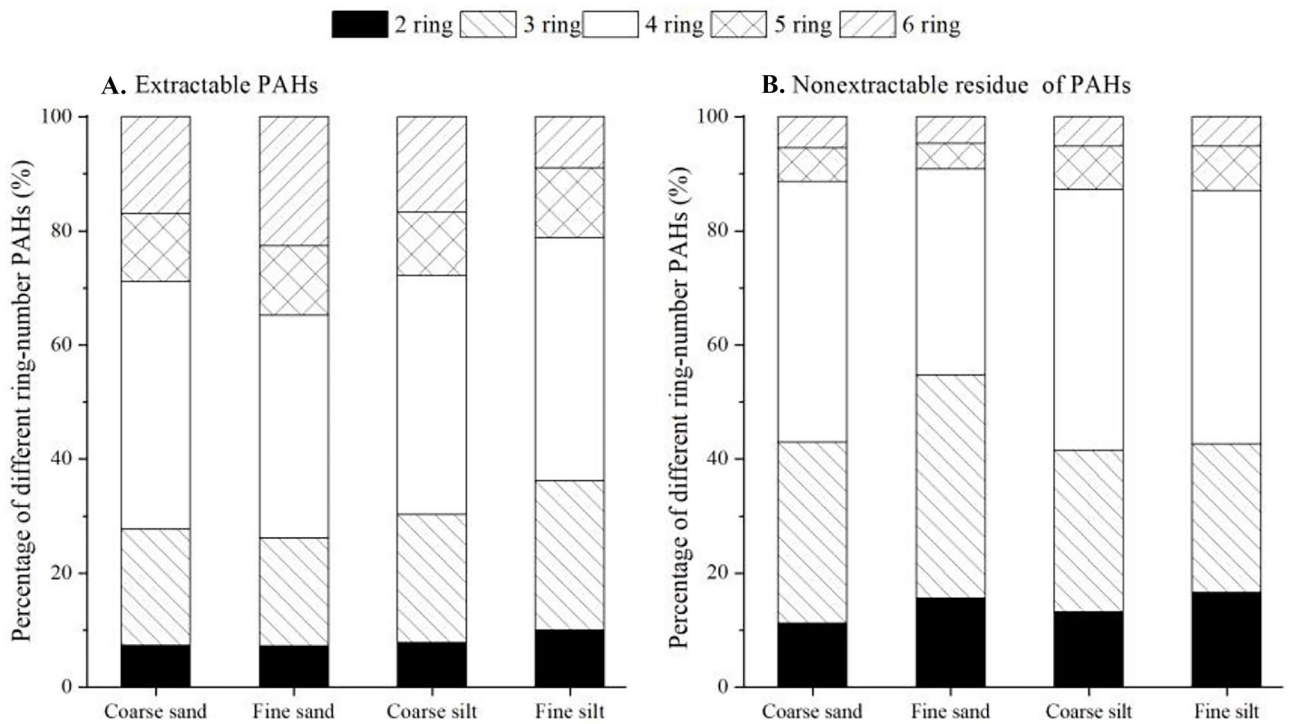

Fig. 3 Compositions of extractable and nonextractable PAHs in particle-size aggregates of Calcareous soil

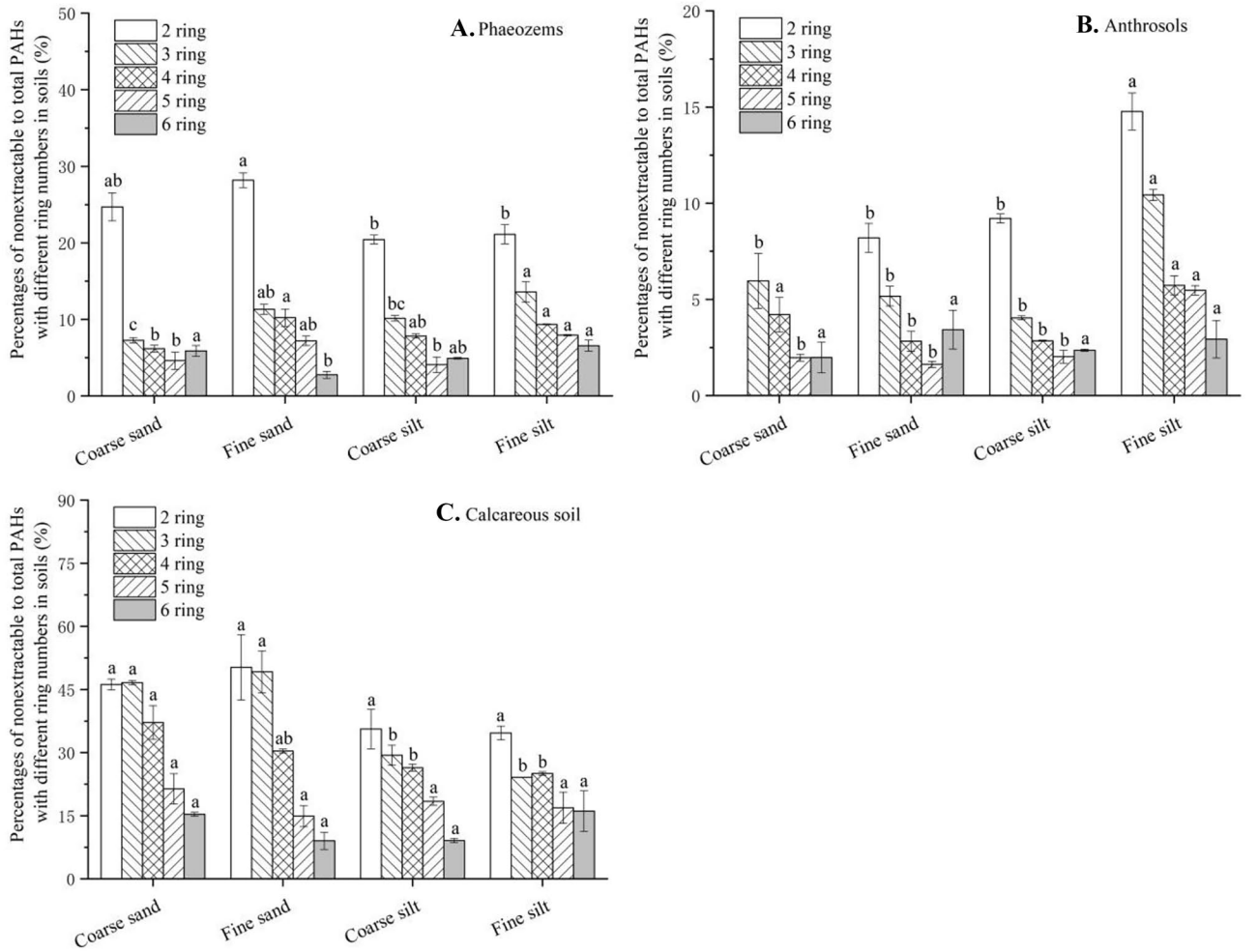

Fig. 4 Proportions of nonextractable PAHs to total PAHs with different ring numbers in soil particle-size aggregates. Different annotated letters above the bars denote the significant differences of PAHs with same ring numbers among particle-size aggregates according to Turkey's test ($p < 0.05$)

rates of other ring-number PAH NERs in all particle-size aggregates were negative. The average degradation rates of PAH NERs in the four particle-size aggregates increased with increasing PAH ring numbers on the whole.

In Anthrosols, the average degradation rates of total PAH NERs in the four particle-size aggregates ranged from 21.1 to 63.2% (Fig. 5B). In respective of different-ring-number PAHs, the average degradation rates of two-ring PAH NERs in all particle-size aggregates and three-ring PAH NERs in coarse silt were negative, and the average degradation rates of other ring-number PAH NERs in all particle-size aggregates were positive. Six-ring PAH NERs were biodegraded completely in all particle-size aggregates except fine silt. Overall, the average degradation rates in the four particle-size aggregates increased with increasing PAH ring numbers.

In Calcareous soil, the average degradation rates of total PAH NERs in the four particle-size aggregates ranged from 23.0 to 55.1% and decreased with decreasing particle size in general (Fig. 5C). In respective of different-ring-number PAHs, there was no consistent trend for the average degradation rates of PAH NERs in all particle-size aggregates.

4 Discussion

4.1 Distribution and formation of nonextractable PAHs in soil particle-size aggregates

In this study, there was no uniform trend for the content of extractable PAHs and PAH NERs and the proportions of PAH NERs in different particle-size aggregates in the three soils (Tables 2, 3, and 4), which might be due to the differences in contamination history, type, and degree and the physico-chemical properties of each soil. Krauss and Wilcke (2002) reported that an accumulation of PAHs in fine sand and silt fractions of soils might be due to the

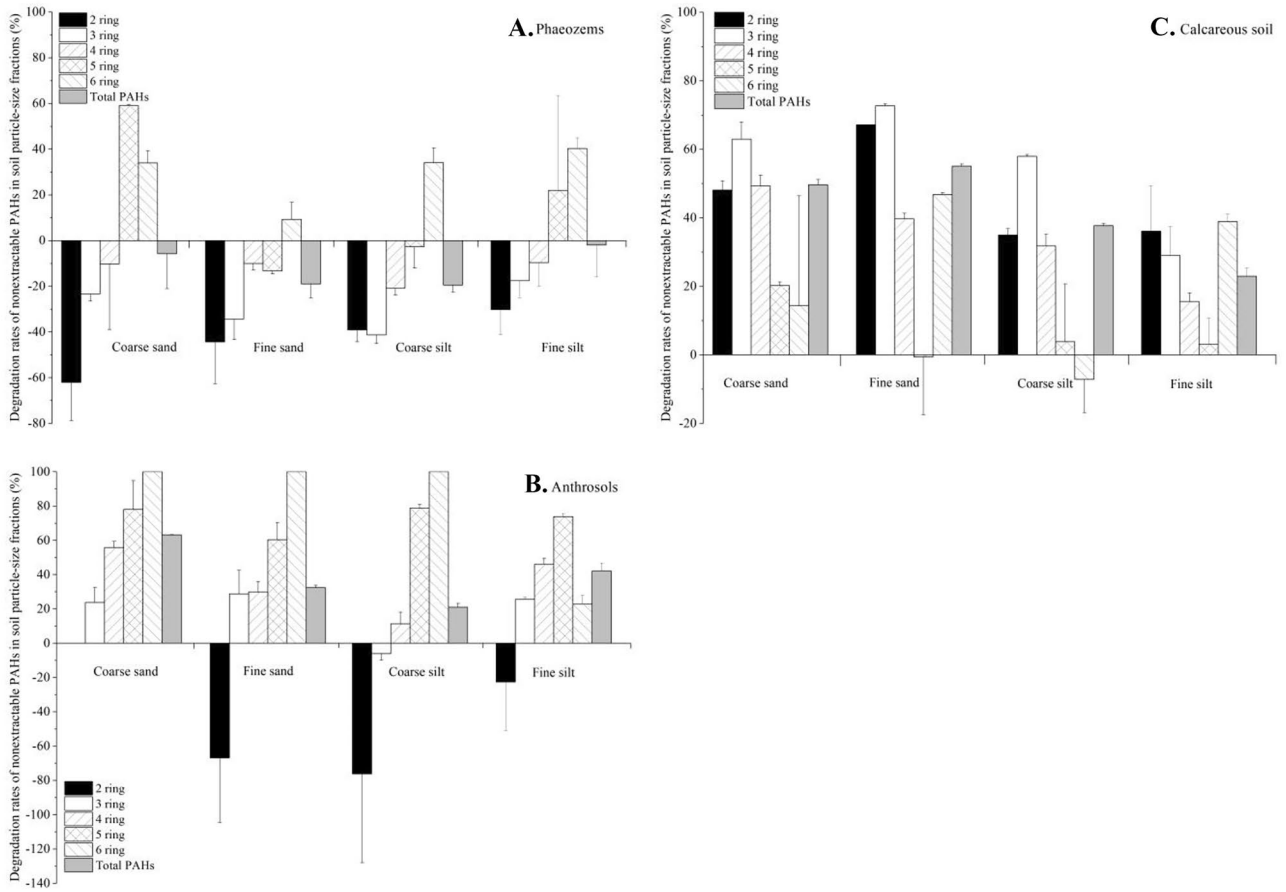

Fig. 5 Biodegradation rates of nonextractable PAHs with different ring numbers in soil particle-size aggregates

main source being the deposition from the atmosphere. Other studies have shown that the sorption of PAHs by SOM increased with increasing aromaticity (Chin et al. 1997; Wilcke et al. 1996; Xing 1997). However, the proportions of two- and three-ring PAHs increased and five- and six-ring PAHs decreased in the composition of PAH NERs in all particle-size aggregates when comparing with the extractable PAHs for every soil (Figs. 1, 2, 3). Furthermore, the average proportion of PAH NERs decreased with the increase of PAH ring numbers in all particle-size aggregates of the three soils in general (Fig. 4). The above results indicated that the molecular size and water solubility of different-ring-number PAHs might affect their NER formation. Large or long molecules can interact concurrently at several points on soil particles, which make them more difficult to migrate into micropores than small or short molecules after being adsorbed (Pignatello and Xing 1996). Additionally, the water solubility of small PAHs is greater than that of large PAHs. Hence, small PAHs can move into more distant interior micropores in soil aggregates than large PAHs and form more NERs. Furthermore, small PAHs were more biodegradable than large PAHs in the extractable form (Haritash and Kaushik 2009). When more extractable small PAHs were biodegraded, the amount of total small PAHs in soil decreased and the proportion of their NERs was accordingly increased based on the calculation formula (1). Thus, the behavior of small PAHs in soil was governed by both biodegradation and NER formation (Ding et al. 2020). Guo et al. (2017) also reported that PAHs with smaller molecular sizes formed more NERs in sediments.

In order to explore the main factors affecting the formation of PAH NERs in soil particle-size aggregates, the data of the three soils was combined to analyze the relationships between soil physico-chemical properties and PAH NERs by Pearson's correlation. Soil organic matter is the main adsorbent for hydrophobic organic compounds in soil (Ukalska-Jaruga et al. 2019). All the contents of PAHs with different ring numbers and total PAHs in soil particle-size aggregates had significantly positive correlations with the contents of OC and TN for both the extractable PAHs and PAH NERs ($p < 0.01$ or $p < 0.05$) (Table S3); however, the content of PAH NERs had a significantly negative correlation with soil C/N ratio ($p < 0.05$) (Table S3). Moreover, the

percentages of PAH NERs to total PAHs in soil particle-size aggregates had no significant correlation with the contents of OC and TN. Thus, the content of SOM was the main factor that controlled the distribution of PAHs in soil particle-size aggregates but not the formation of PAH NERs.

It is believed that NERs of organic chemicals can be formed in the soil through physical entrapment and chemical bonding (Loiseau and Barriuso 2002). Since the parent PAH compounds do not possess any coupling groups, they can form PAH NERs through physical trapping (sequestration) and chemical interactions including van der Waals forces, charge-transfer complexes, and hydrophobic partitioning (Burauel and Führ 2000; Craven 2000; Mordaunt et al. 2005). From Table S4, all the percentages of PAH NERs to total PAHs in soil particle-size aggregates for different-ring-number PAH NERs and total PAH NERs had significantly positive correlations with SSA and pore parameters (e.g., micro-, meso-, and macropore area and volume) except two-ring PAHs. The percentages of two-ring PAH NERs had no significant correlation with macropore area and volume, which indicated that two-ring PAHs were not easily sequestered in macropores due to their smaller molecular size and higher water solubility than other PAHs. The above results suggested that physical trapping was the main factor that controlled the formation of PAH NERs in soil particle-size aggregates and two-ring PAH NERs were mainly in micro- and meso-pores.

4.2 Biodegradation of nonextractable PAHs in soil particle-size aggregates

The biodegradation rates of PAH NERs in the different particle-size aggregates were different in each soil and there was no consistent trend in all three soils (Fig. 5). The biodegradation rates of PAH NERs in all particle-size aggregates were lower in Phaeozems than those in Anthrosols and Calcareous soil, which might due to the higher OC contents and proportions of micropores in Phaeozems (Table 1, Table S1). The biodegradation rates of some PAH NERs were negative in particle-size aggregates of the three soils (Fig. 5), which meant that the amount of these PAH NERs in soils increased after biodegradation instead of decreasing. The increase of these PAH compounds in particle-size aggregates after biodegradation experiments might be from microbial production. Wakeham et al. (1980) reported that some PAHs were abundant in very young sediment layers and might be derived by microbially mediated transformations of biogenic precursors. A microcosm experiment suggested that Nap can be produced by fungi and bacteria associated with termites (Musa Bandowe et al. 2009). Nap and Phe had been reported as intermediates during the biodegradation of Pyr and BaP in some studies (Abo-State et al. 2021; Li et al. 2018; Liang et al. 2014; Xu et al. 2022). On the other hand, the increase of these PAHs might also be caused by measurement error due to the complex pretreatment of quantifying PAHs.

The results of correlation analysis showed that the biodegradation rates of total PAH NERs were significantly negatively correlated with OC ($p < 0.05$) and TN ($p < 0.01$) in soil particle-size aggregates (Table S5); however, there was no significant correlation between the biodegradation rates of total PAH NERs and SSA and pore parameters (e.g., A_{micro}, A_{meso}, A_{macro}, A_{total}, V_{micro}, V_{meso}, V_{macro}, V_{total}). Thus, the biodegradation rates of total PAH NERs were mainly determined by the content of SOM in particle-size aggregates. In respective of different-ring-number PAHs, the degradation rate of four-ring PAH NERs had a significantly negative correlation with OC and TN ($p < 0.05$). The degradation rate of five-ring PAH NERs had a significantly negative correlation with SSA, A_{micro}, and V_{micro} ($p < 0.05$) (Table S5). The results indicated that biodegradation rates of some high-molecular-weight PAH NERs were hindered by the sorption of SOM and/or occlusion in micropores. Soil organic matter is the main adsorbent for PAHs in soil (Ukalska-Jaruga et al. 2019) and the molecules of high-molecular-weight PAHs can interact simultaneously at multiple points on soil particles (Pignatello and Xing 1996), which make them adsorb tightly on soil particles and reduce their biodegradability. Moreover, once the molecules of high-molecular-weight PAHs entered soil micropores, their bioaccessibility was restricted and the biodegradation rates decreased accordingly. By contrast, the degradation rates of two-ring and three-ring PAH NERs in different particle-size aggregates were significantly positively correlated with SSA and pore parameters (e.g., A_{micro}, A_{meso}, A_{macro}, A_{total}, V_{micro}, V_{meso}, V_{macro}, V_{total}) ($p < 0.05$ or 0.01) (Table S5). Two-ring and three-ring PAH NERs were formed mainly through sequestration; more pore structures in soil particle-size aggregates caused more NER formation. During the biodegradation experiments, the pore structure in soil particle-size aggregates might be collapsed or changed and the two-ring and three-ring PAH NERs were then exposed. When the contents of the two-ring and three-ring PAH NERs were higher in soil particle-size fractions, their exposure and biodegradation probability were also higher, and thus the biodegradation rates were increased consequently.

5 Conclusions

The percentages of PAH NERs to total PAHs in soil particle-size aggregates were in the range of 6.7–9.8%, 2.8–6.0%, and 24.3–35.9% for Phaeozems, Anthrosols, and Calcareous soil, respectively. Four-ring PAHs were generally the dominant PAHs in the compositions of the extractable PAHs and PAH NERs in all particle-size aggregates for the three

soils. Comparing with the extractable PAHs, the proportions of two- and three-ring PAHs increased and five- and six-ring PAHs decreased in the composition of PAH NERs in all particle-size aggregates for every soil on the whole. Moreover, the average proportion of PAH NERs decreased with the increase of PAH ring numbers in all particle-size aggregates of the three soils in general. The contents of the extractable PAHs and PAH NERs in soil particle-size aggregates had significantly positive correlations with the contents of OC and TN ($p < 0.01$ or $p < 0.05$). The proportions of PAH NERs in soil particle-size aggregates had significantly positive correlations with SSA and pore parameters (e.g., micro-, meso-, and macropore area and volume) in general ($p < 0.01$ or $p < 0.05$). Due to the higher OC contents and proportions of micropores, the biodegradation rates of PAH NERs in all particle-size aggregates of Phaeozems were lower than those of Anthrosols and Calcareous soil.

The results in this study indicated that the distribution and formation of PAH NERs in soil particle-size aggregates were mainly controlled by different soil physico-chemical properties, which helped to deeply understand the environmental fates of PAHs in field-contaminated soils.

Supplementary Information The online version contains supplementary material available at https://doi.org/10.1007/s11368-023-03578-9.

Funding This work was supported by the National Natural Science Foundation of China (42077130) and the Natural Science Foundation of Fujian Province (2020J01189 and 2020J01140).

Data availability All data included in this study are available upon request by contact with the corresponding author.

Declarations

Competing interests The authors declare no competing interests.

References

Abo-State MAM, Osman ME, Khattab OH, El-Kelani TA, Abdel-Rahman ZM (2021) Degradative pathways of polycyclic aromatic hydrocarbons (PAHs) by *Phanerochaete chrysosporium* under optimum conditions. J Radiat Res Appl Sc 14(1):507–520. https://doi.org/10.1080/16878507.2021.2001247

Alexander M (2000) Aging, bioavailability, and overestimation of risk from environmental pollutants. Environ Sci Technol 34(20):4259–4265. https://doi.org/10.1021/es001069+

Amelung W, Zech W, Zhang X, Follett RF, Tiessen H, Knox E, Flach KW (1998) Carbon, nitrogen, and sulfur pools in particle-size fractions as influenced by climate. Soil Sci Soc Am J 62(1):172–181. https://doi.org/10.2136/sssaj1998.03615995006200010023x

Berry DF, Boyd SA (1985) Decontamination of soil through enhanced formation of bound residues. Environ Sci Technol 19(11):1132–1133. https://doi.org/10.1021/es00141a020

Birdwell JE, Thibodeaux LJ (2009) PAH repartitioning in field-contaminated sediment following removal of the labile chemical fraction. Environ Sci Technol 43(21):8092–8097. https://doi.org/10.1021/es9016798

Bol R, Poirier N, Balesdent J, Gleixner G (2009) Molecular turnover time of soil organic matter in particle-size fractions of an arable soil. Rapid Commun Mass Spectrom 23:2551–2558. https://doi.org/10.1002/rcm.4124

Burauel P, Führ F (2000) Formation and long-term fate of nonextractable residues in outdoor lysimeter studies. Environ Pollut 108(1):45–52. https://doi.org/10.1016/s0269-7491(99)00200-6

Chin YP, Aiken GR, Danielsen KM (1997) Binding of pyrene to aquatic and commercial humic substances: the role of molecular weight and aromaticity. Environ Sci Technol 31(6):1630–1635. https://doi.org/10.1021/es960404k

Costera A, Feidt C, Dziurla MA, Monteau F, Bizec BL, Rychen G (2009) Bioavailability of polycyclic aromatic hydrocarbons (PAHs) from soil and hay matrices in lactating goats. J Agric Food Chem 57(12):5352–5357. https://doi.org/10.1021/jf9003797

Craven A (2000) Bound residues of organic compounds in the soil: the significance of pesticide persistence in soil and water: a European regulatory view. Environ Pollut 108(1):15–18. https://doi.org/10.1016/S0269-7491(99)00198-0

Ding Y, Li Li, Wania F, Zhang Y, Huang H, Liao T, Liu J, Qi S (2020) Formation of non-extractable residues as a potentially dominant process in the fate of PAHs in soil: insights from a combined field and modeling study on the eastern Tibetan Plateau. Environ Pollut 267:115383. https://doi.org/10.1016/j.envpol.2020.115383

Doick KJ, Burauel P, Jones KC, Semple KT (2005) Distribution of aged ^{14}C-PCB and ^{14}C-PAH residues in particle-size and humic aggregates of an agricultural soil. Environ Sci Technol 39(17):6575–6583. https://doi.org/10.1021/es050523c

Duan L, Palanisami T, Liu YJ, Dong ZM, Mallavarapu M, Kuchel T, Semple KT, Naidu R (2014) Effects of ageing and soil properties on the oral bioavailability of benzo[a]pyrene using a swine model. Environ Int 70:192–202. https://doi.org/10.1016/j.envint.2014.05.017

Eschenbach A, Wienberg R, Mahro B (1998) Fate and stability of nonextractable residues of [^{14}C]PAH in contaminated soils under environmental stress conditions. Environ Sci Technol 32(17):2585–2590. https://doi.org/10.1021/es9708272

Gao Y, Hu X, Zhou Z, Zhang W, Wang Y, Sun B (2017) Phytoavailability and mechanism of bound PAH residues in field contaminated soils. Environ Pollut 222:465–476. https://doi.org/10.1016/j.envpol.2016.11.076

Gao Y, Wang Y, Zeng Y, Zhu X (2013) Phytoavailability and rhizospheric gradient distribution of bound-polycyclic aromatic hydrocarbon residues in soils. Soil Sci Soc Am J 77(5):1572–1583. https://doi.org/10.2136/sssaj2013.04.0128

Guidi P, Falsone G, Wilson C, Cavani L, Ciavatta C, Marzadori C (2021) New insights into organic carbon stabilization in soil macroaggregates: an in situ study by optical microscopy and SEM-EDS technique. Geoderma 397:115101. https://doi.org/10.1016/j.geoderma.2021.115101

Guo JY, Chen JA, Wang JF, Wu FC (2017) Bound PAHs in sediment and related environmental significance. Arch Environ Con Tox 72(4):530–539. https://doi.org/10.1007/s00244-017-0393-x

Haritash AK, Kaushik CP (2009) Biodegradation aspects of polycyclic aromatic hydrocarbons (PAHs): a review. J Hazard Mater 169(1–3):1–15. https://doi.org/10.1016/j.jhazmat.2009.03.137

Khan MI, Cheema SA, Shen C, Zhang C, Tang X, Shi J, Chen X, Park J, Chen Y (2012) Assessment of phenanthrene bioavailability in aged and unaged soils by mild extraction. Environ Monit Assess 184(1):549–559. https://doi.org/10.1007/s10661-011-1987-9

Krauss M, Wilcke W (2002) Sorption strength of persistent organic pollutants in particle-size aggregates of urban soils. Soil Sci Soc Am J 66(2):430–437. https://doi.org/10.2136/sssaj2002.0430

Ling W, Zeng Y, Gao Y, Dang H, Zhu X (2010) Availability of polycyclic aromatic hydrocarbons in aging soils. J Soils Sediments 10(5):799–807. https://doi.org/10.1007/s11368-010-0187-5

Li N, Long J, Han X, Yuan Y, Sheng M (2020) Molecular characterization of soil organic carbon in water-stable aggregate aggregates during the early pedogenesis from parent material of Mollisols. J Soils Sediments 20(4):1869–1880. https://doi.org/10.1007/s11368-020-02563-w

Li X, Zhang X, Li L, Lin C, Dong W, Shen W, Yong X, Jia H, Wu X, Zhou J (2018) Anaerobic biodegradation of pyrene by *Klebsiella* sp. LZ6 and its proposed metabolic pathway. Environ Technol 41(16):2130–2139. https://doi.org/10.1080/09593330.2018.1556348

Liang A, Zhang Y, Zhang X, Yang X, McLaughline N, Chen X, Guo Y, Jia S, Wang L, Tang J (2019) Investigations of relationships among aggregate pore structure, microbial biomass, and soil organic carbon in a Mollisol using combined non-destructive measurements and phospholipid fatty acid analysis. Soil till Res 185:94–101. https://doi.org/10.1016/j.still.2018.09.003

Liang L, Song X, Kong J, Shen C, Huang T, Hu Z (2014) Anaerobic biodegradation of high-molecular-weight polycyclic aromatic hydrocarbons by a facultative anaerobe *Pseudomonas* sp. JP1. Biodegradation 25:825–833. https://doi.org/10.1007/s10532-014-9702-5

Liao X, Ma D, Yan X, Yang L (2013) Distribution pattern of polycyclic aromatic hydrocarbons in particle-size aggregates of coking plant soils from different depth. Environ Geochem Hlth 35(3):271–282. https://doi.org/10.1007/s10653-012-9482-y

Loiseau L, Barriuso E (2002) Characterization of the atrazine's bound (nonextractable) residues using fractionation techniques for soil organic matter. Environ Sci Technol 36(4):683–689. https://doi.org/10.1021/es010146d

Lu Z, Zeng F, Xue N, Li F (2012) Occurrence and distribution of polycyclic aromatic hydrocarbons in organo-mineral particles of alluvial sandy soil profiles at a petroleum-contaminated site. Sci Total Environ 433:50–57. https://doi.org/10.1016/j.scitotenv.2012.06.036

Maqsood S, Murugan R (2017) Distribution of persistent organic pollutants in aggregate aggregates of a temperate forest and semi-rural soil. J Forestry Res 28(5):953–961. https://doi.org/10.1007/s11676-017-0380-0

Mordaunt CJ, Gevao B, Jones KC, Semple KT (2005) Formation of non-extractable pesticide residues: observations on compound differences, measurement and regulatory issues. Environ Pollut 133(1):25–34. https://doi.org/10.1016/j.envpol.2004.04.018

Musa Bandowe BA, Ruckamp D, Braganca MAL, Laabs V, Amelung W, Martius C, Wilcke W (2009) Naphthalene production by microorganisms associated with termites: evidence from a microcosm experiment. Soil Biol Biochem 41(3):630–639. https://doi.org/10.1016/j.soilbio.2008.12.029

Ni JZ, Luo YM, Wei R, Li XH (2008) Distribution of polycyclic aromatic hydrocarbons in particle-size separates and density aggregates of typical agricultural soils in the Yangtze River Delta, east China. Eur J Soil Sci 59(6):1020–1026. https://doi.org/10.1111/j.1365-2389.2008.01066.x

Pignatello JJ, Xing BS (1996) Mechanisms of slow sorption of organic chemicals to natural particles. Environ Sci Technol 30(1):1–11. https://doi.org/10.1021/es940683g

Ray S, Khillare PS, Kim KH, Brown RJ (2012) Distribution, sources, and association of polycyclic aromatic hydrocarbons, black carbon, and total organic carbon in size-segregated soil samples along a background–urban–rural transect. Environ Eng Sci 29(11):1008–1019. https://doi.org/10.1089/ees.2011.0323

Regelink IC, Stoof CR, Rousseva S, Weng L, Lair GJ, Kram P, Nikolaidis NP, Kercheva M, Banwart S, Comans RNB (2015) Linkages between aggregate formation, porosity and soil chemical properties. Geoderma 247–248:24–37. https://doi.org/10.1016/j.geoderma.2015.01.022

Richnow HH, Annweiler E, Koning M, Lüth JC, Stegmann R, Garms C, Francke W, Michaelis W (2000) Tracing the transformation of labelled [1-^{13}C] phenanthrene in a soil bioreactor. Environ Pollut 108(1):91–101. https://doi.org/10.1016/S0269-7491(99)00205-5

Schulten HR, Leinweber P (2000) New insights into organic-mineral particles: composition, properties and models of molecular structure. Biol Fertil Soils 30(5–6):399–432. https://doi.org/10.1007/s003740050020

Ukalska-Jaruga A, Smreczak B, Klimkowicz-Pawlas A (2019) Soil organic matter composition as a factor affecting the accumulation of polycyclic aromatic hydrocarbons. J Soils Sediments 19(4):1890–1900. https://doi.org/10.1007/s11368-018-2214-x

Umeh AC, Duan L, Naidu R, Semple KT (2018a) Time-dependent remobilisation of non-extractable benzo[a]pyrene residues in contrasting soils: effects of aging, spiked concentration, and soil properties. Environ Sci Technol 52(21):12295–12305. https://doi.org/10.1021/acs.est.8b03008

Umeh AC, Duan L, Naidu R, Semple KT (2018b) Enhanced recovery of nonextractable benzo[a]pyrene residues in contrasting soils using exhaustive methanolic and nonmethanolic alkaline treatments. Anal Chem 90(21):13104–13111. https://doi.org/10.1021/acs.analchem.8b04440

Wakeham SG, Schaffner C, Giger W (1980) Polycyclic aromatic hydrocarbons in Recent lake sediments — II. Compounds derived from biogenic precursors during early diagenesis. Geochimica Et Cosmochimica Acta 44(3):415–429. https://doi.org/10.1016/0016-7037(80)90041-1

Wang Y, Xu J, Shan J, Ma Y, Ji R (2017) Fate of phenanthrene and mineralization of its non-extractable residues in an oxic soil. Environ Pollut 224:377–383. https://doi.org/10.1021/10.1016/j.envpol.2017.02.017

Wild SR, Jones KC (1995) Polynuclear aromatic hydrocarbons in the United Kingdom environment: a preliminary source inventory and budget. Environ Pollut 88(1):91–108. https://doi.org/10.1016/0269-7491(95)91052-M

Wilcke W, Zech W, Kobža J (1996) PAH-pools in soils along a PAH-deposition gradient. Environ Pollut 92(3):307–313. https://doi.org/10.1016/0269-7491(95)00110-7

Xing B (1997) The effect of the quality of soil organic matter on sorption of naphthalene. Chemosphere 35:633–642. https://doi.org/10.1016/S0045-6535(97)00125-2

Xu M, Wu M, Zhang Y, Zhang H, Guo L (2022) Biodegradation of polycyclic aromatic hydrocarbons (PAHs) by bacterial mixture. Int J Environ Sci Te 19:3833–3844. https://doi.org/10.1007/s13762-021-03284-4

Yang M, Wei R, Chen W, Yang L, Ni J (2023) Distribution patterns, toxic equivalence, and environmental risks of polycyclic aromatic hydrocarbons in different density fractions of long-term field-contaminated soils. J Soils Sediments 23:1370–1380. https://doi.org/10.1007/s11368-022-03391-w

Publisher's Note Springer Nature remains neutral with regard to jurisdictional claims in published maps and institutional affiliations.

Springer Nature or its licensor (e.g. a society or other partner) holds exclusive rights to this article under a publishing agreement with the author(s) or other rightsholder(s); author self-archiving of the accepted manuscript version of this article is solely governed by the terms of such publishing agreement and applicable law.